

Novel Fabrication of Renewable Aerogels from Coconut Coir Fibers for Dye Removal

Nguyen Tran Xuan Phuong^{a,d}, Kim H. Ho^{a,b}, Chi Thi Xuan Nguyen^{a,b}, Yen Tieu Dang^{a,b}, Nga Hoang Nguyen Do^{a,b}, Kien Anh Le^c, Tai Chiem Do^d, Phung Thi Kim Le^{a,b,*}

^a Faculty of Chemical Engineering, Ho Chi Minh City University of Technology (HCMUT), 268 Ly Thuong Kiet Street, District 10, Ho Chi Minh City, Vietnam

^b Vietnam National University Ho Chi Minh City, Linh Trung Ward, Thu Duc District, Ho Chi Minh City, Vietnam

^c Institute for Tropicalization and Environment, 57A Truong Quoc Dung Street, Phu Nhuan District, Ho Chi Minh City, Vietnam

^d Hong Bang International University (HIU), 215 Dien Bien Phu Street, Ward 15, Binh Thanh District, Ho Chi Minh City, Vietnam
 phungle@hcmut.edu.vn

Water pollution resulted from the discharge of the textile industry limits light penetration into the water, negatively affects the photosynthesis of aquatic organisms, and causes serious risks of cancer and genetic mutation for humans living near the emission site. The utilization of porous materials like aerogels to adsorb dye has been one of the effective methods for wastewater treatment. The fabrication of renewable materials from agricultural waste both to take advantage of its abundance and increase its value has gained research interest in recent years. In this research, this is the first time natural cellulose aerogel from coconut fibers (CFs) have successfully been developed by physically cross-linking cellulose with non-toxic binders including polyvinyl alcohol (PVA) and xanthan gum (XTG) in distilled water, followed by cost-effective freeze-drying to sublimate water and leave the hollow structure. The as-fabricated cellulose aerogel exhibits a tremendously low density (0.041 g/cm^3) and high porosity (96.30 %). The aerogels are then tested for methylene blue (MB) adsorption in water to evaluate its applicability in the treatment of dye-contaminated water with varied investigated factors such as contact time, pH values, and MB initial concentrations. The MB adsorption process of the aerogels reaches equilibrium after 50 min and their adsorption isotherms follow the Freundlich model with an R-square value of 0.9453. It is worth noting that the highest adsorption capacity of the synthesized aerogels is up to 11.84 mg/g when the initial MB concentration is 25 mg/L at pH 7. The feasible procedure to synthesize recycled cellulose aerogels from CFs with green chemicals in this study has created good promise for dye adsorbents. About the potential economic benefits, the CFs are abundant agricultural wastes, easy pretreated processing involved in saving energy costs.

1. Introduction

Because of the rapid growth of textile, pharmaceutical, printing, food, paint, and cosmetics, the elimination of dye-contaminated water has been one of the most environmental degradations that Vietnam and other developing countries are facing. MB is a cationic dye, medicine, and may cause poison at over-concentration (greater than 100 mg/kg). Its molecule is difficult to break down under natural conditions, its existence in water can cause serious problems for living species and human health (Ben et al., 2020). To remove MB from industrial effluents, using highly porous aerogels as an adsorbent is known as an effective and successful technique.

During the New Material Revolution, one of the most significant achievements is aerogel having a hollow porous network by replacing a liquid in a gel with a gas. Cellulose is a natural raw material that is plentiful, inexpensive, renewable, and bio-hydrolytic. Natural cellulosic aerogel is one of the remarkable materials with numerous benefits such as high biocompatibility, high bulk porosity, low density, great surface area which has promise in the treatment of environmental problems, particularly water pollution (Nga et al., 2021).

Coconut trees ranked seventh in terms of land area in 93 countries in the world and ranked fourth among perennial industrial trees in Vietnam (Minh and Trong, 2019). By 2025, the average demand for coconut products such as coconut milk, organic coconut milk, coconut jelly, coconut meal, coconut cream, coconut water, and coconut oil will rise globally by 10 % (Hiep, 2018). Almost parts of the tree are utilized to construct houses, make handicrafts, and household items such as chopsticks, tables, shelves, weaving carpets to name a few. Scientists are interested in CFs which are raw, hard, reddish-brown filament obtained from the outer shell of the coconut. Because of the high biodegradable cellulose content (23 – 43 %), low cost, and abundance, the CFs are one of the potential candidates to develop cellulose-based aerogels (Mar'atul et al., 2019).

Over the past decades, scientists have studied and prepared cellulose aerogels from different sources, for example, sugarcane bagasse (Quoc et al., 2020), pineapple leaf/cotton waste fibers composites (Nga et al., 2021), or cigarette butts (Ngoc et al., 2020). To dissolve cellulose, dimethyl sulfoxide/lithium chloride (DMSO/LiCl) (Zhigu et al., 2012), NaOH/urea solvent (Mar'atul et al., 2019) have also been proposed. As can be observed, there are lots of different methods to dissolve cellulose aerogels but some disadvantages such as expensive, DMSO contains sulfur, poisonousness, and volatilization. In recent times, a bio-aqueous solution containing PVA/XTG as an effective crosslinker has been also developed towards sustainable and eco-friendly criteria. In this paper, for the first time, a renewable aerogel is fabricated from CFs with PVA/XTG through sol-gel, aging, and freeze-drying process. The adsorption properties of developed CFs aerogel on the cationic dye MB are evaluated by various batch experiments.

2. Experimental methods

2.1 Materials

CFs were obtained from the factory in Ben Tre province (Vietnam) with a diameter of about 125 μm . MB (99.5 wt%) was purchased from Xilong. PVA (85-124 kDa) and XTG (4,500 kDa) flakes were obtained from Sigma-Aldrich.

2.2 Fabrication of CFs aerogel

The ground CFs were digested in an alkali solution using 6.0 wt% NaOH with a solid-to-liquid ratio of 1:20 g/mL, heated at 90 $^{\circ}\text{C}$ for 4 h. The obtained fibers were filtrated, rinsed until neutral pH by distilled water before further drying in the oven at 80 $^{\circ}\text{C}$ for 24 h. The pretreated CFs were ground, sieved with approx. 50-125 μm in diameter, and used for fabrication of CFs aerogel.

To obtain the CFs aerogel, PVA and XTG were used as the binders, 0.60 wt% PVA and 0.30 wt% XTG solvent was dissolved by 0.30 g of PVA and 0.15 g of XTG in 50 mL demineralized water at 80 $^{\circ}\text{C}$ under magnetic stirring. Next step, 0.15 g pretreated CFs were dispersed into the PVA/XTG solution. To homogenize and remove air, the mixture was subsequently ultrasound-assisted for 15 min. The aging process was conducted in the oven at 70 $^{\circ}\text{C}$ and maintained for 2 h to promote the connection between PVA/XTG cross-linker and CFs. The cellulose suspension was gelation at -4 $^{\circ}\text{C}$ for 24 h before being freeze-dried by A Toption TPV-50F vacuum freeze dryer (at 5 Pa for 48 h). Finally, CFs aerogel was preserved in a desiccator for further experiments.

2.3 Characterization

The bulk density of recycled CFs aerogel was obtained by measuring the volume and weight of the cylinder-shaped material. The porosity, φ (%) of each sample was determined by Eq(1) (Luu et al., 2020).

$$\varphi = \left(1 - \frac{\rho_a}{\rho_b}\right) \times 100 \quad (1)$$

$$\rho_b = \frac{C_{CF} + C_{PVA} + C_{XTG}}{\frac{C_{CF}}{\rho_{CF}} + \frac{C_{PVA}}{\rho_{PVA}} + \frac{C_{XTG}}{\rho_{XTG}}} \quad (2)$$

where ρ_a (g/cm^3) is the density of aerogel and ρ_b is average density of components determined by Eq(2). ρ_{CF} (1.2 g/cm^3), ρ_{PVA} (1.2 g/cm^3), ρ_{XTG} (1.5 g/cm^3) are the density of the CFs, PVA, and XTG. C_{CF} , C_{PVA} , C_{XTG} are the contents of the CFs, PVA, and XTG.

The surface morphology of CFs aerogel was carried out on a Field-Emission Scanning Electron Microscope (FE-SEM S4800). The sample was coated with a thin platinum layer for 30 s by a sputtering coater before measurement. The Fourier transform infrared spectra (FT-IR) was performed on a Bruker FT-IR spectrometer (Germany) in the scanned range of 4,000–400 cm^{-1} using KBr as a matrix.

To determine the point of zero charge (pH_{zpc}) of CFs aerogel, 25 mL NaCl solution (0.1 M) was adjusted the initial pH from 3 to 11 by 0.1 M HCl or NaOH solutions. 50 mg CFs aerogel was added, and the mixtures were

equilibrated for 48 h. The difference between the initial and final pH ($\Delta\text{pH} = \text{pH}_f - \text{pH}_i$) compared with the initial pH was a curve. The intersection of this curve and the straight line passing through origin was the pH_{pzc} value.

2.4 Adsorption experiment

Adsorption experiments are designed to survey the interaction time (10-70 min), pH (3-11), and initial dye concentration (12.5 - 100 mg/L) on the MB adsorption capacity of the CFs aerogel. Briefly, 50 mg of adsorbent was immersed in 20 mL of MB solution at room temperature. After a fixed adsorption time, the remaining amount of MB in the aqueous solutions was analysed by the Agilent Cary 60 UV-Vis spectrophotometer at a wavelength of 640 nm. The adsorption capacity, q_e (mg/g) and removal efficiency, H % of CFs aerogel were calculated by the following Eqs(3) and (4) (Su et al., 2020).

$$q_e = \frac{(C_0 - C_e) \cdot V}{m} \quad (3)$$

$$\text{H \%} = \frac{(C_0 - C_e)}{C_0} \times 100 \quad (4)$$

where C_0 and C_e (mg/L) are the initial and final MB concentration. V (L) is the volume of MB solution, and m (g) was the weight of the CFs aerogel before adsorption.

Both linearized kinetic models, namely the pseudo-first-order and pseudo-second-order models, are expressed based on the following Eqs(5) and (6) (Etim et al., 2016).

$$\ln(q_e - q_t) = \ln q_e - k_1 t \quad (5)$$

$$\frac{t}{q_t} = \frac{1}{k_2 \cdot q_e^2} + \frac{1}{q_e} \cdot t \quad (6)$$

where q_e and q_t are the adsorption capacities of CFs aerogel at equilibrium and at time t (mg/g); k_1 and k_2 represent the kinetic rate constants for pseudo-first-order and pseudo-second-order models.

The Langmuir and Freundlich isotherm models were chosen to research sorption mechanisms and maximum adsorption capacity of the CFs aerogel. The calculation methods of the two common models are shown in Eqs(7) and (8) (Etim et al., 2016), where the equilibrium constants k_L , k_F are fitted for Langmuir and Freundlich models; q_{max} is the maximum adsorption capacity of CFs aerogel for MB (mg/g).

$$\frac{C_e}{q_e} = \frac{C_e}{q_{\text{max}}} + \frac{1}{k_L q_{\text{max}}} \quad (7)$$

$$\ln q_e = \ln k_F + \frac{\ln C_e}{n} \quad (8)$$

The calculation of the Gibbs free energy (ΔG) was determined by Eq(9) (Etim et al., 2016), where K is obtained of the linear plot of $\ln C_s/C_e$ against C_s , C_s is adsorbent MB concentration (mg/g), R is the universal gas constant (8.314 J/mol K); T is the MB solution's temperature (303 K).

$$\Delta G = -RT \ln K \quad (9)$$

3. Results and discussion

3.1 Characterization of the CFs aerogel

3.1.1 Physicochemical properties

A challenging field of study is the synthesis of biocomposite materials in connection with biodegradability, morphology-controlled synthesis, formation mechanisms, or advanced properties. In this paper, a novel fabrication of aerogel uses renewable cellulose from CFs, green and bio-solvent via sol-gel, aging, and vacuum freeze-drying process. A liquid is mainly eliminated by sublimation after the gel is frozen below the freezing temperature of the water, which is an important condition in avoiding structural break-down and reducing shrinkage (Nga et al., 2021) The fabricated CFs aerogel exhibits an enormously low density (0.041 g/cm³) and possesses a high porosity (96.30 %) indicating its lightweight and porous structure. The morphology of aerogel is shown in Figure 1a confirming its open porous network without the discernible organization of CFs indicating that it is successfully synthesized from treated CFs by the developed procedure.

The pH_{zpc} confirms the chemical property of the CFs aerogel surface, which equals 6.8. This result indicates that the adsorbent's surface has been positively charged at $pH < 6.8$, neutral at $pH 6.8$, and negatively charged at $pH > 6.8$.

3.1.2 FT-IR analysis

Figure 1b shows the FTIR spectra of pretreated CFs and the as-fabricated aerogel. The broad absorption band at around $3,575\text{ cm}^{-1}$ represents of O-H stretching vibration of hydroxyl groups (Mar'atul et al., 2019). The absorption band at $2,900\text{ cm}^{-1}$ is originated from sp^3 -CH stretching vibration involved in methyl groups. An intensified and overlapped peak of about $1,737\text{ cm}^{-1}$ is assigned to the acetyl groups of hemicellulose and the carbonyl groups in native lignin structure. The absorption band at a wavenumber of $1,657\text{ cm}^{-1}$ is supposed C=O stretching. While the peak around $1,514\text{ cm}^{-1}$ indicates the ring stretching vibration of aromatic C=C in lignin, the band located at $1,265\text{ cm}^{-1}$ is the stretching vibration of acetyl groups in hemicellulose. The skeletal deformation of pyranose rings ($1,054\text{ cm}^{-1}$) and rocking vibrations of C-H (897 cm^{-1}) have been associated with the typical characteristic of natural cellulose (Quoc et al., 2020).

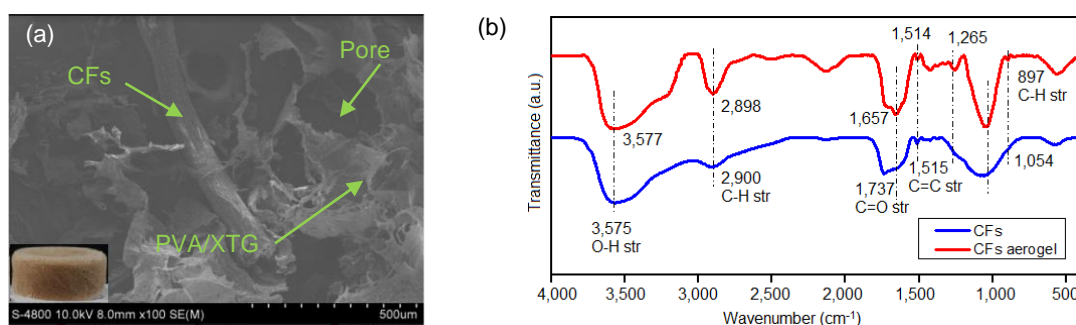


Figure 1: (a) FE-SEM images, (b) FTIR spectra of pretreated CFs and CFs aerogel

3.2 MB absorption capability of the CFs aerogel

3.2.1 Contact time

The adsorption equilibrium time is a significant factor in the evaluation of the adsorbent, which immediately affects the adsorption efficiency of the adsorbent. The interaction time of both CFs aerogel and MB molecules on the adsorption efficiency is surveyed. As shown in Figure 2a, with the initial concentration of 25 mg/L the adsorption capability of CFs aerogel is a rising function with contact time. The MB removal increases rapidly in the first 10 min (from 0 to 72.32 %) and reached constant values after 50 min (approximately 92 % and 23 mg/g). The colorant adsorption of CF aerogel tends to increase slightly when the contact time is in the range of 10-50 min since the mass transfer of MB molecules decreases as the pores inside become narrower. After 50 min, the adsorption seems to reach equilibrium because the adsorption sites on the aerogel's surface are filled with MB, thus 50 min is chosen for further adsorption studies of CF aerogels.

3.2.2 pH

The effect of pH is extremely essential in adsorption of investigation particularly dye adsorption. The pH solution controls the magnitude of electrostatic charges which are caused by the ionized dye molecules and the charges on the CFs aerogel's surface. The pH of an aqueous medium changes the adsorption capacity of the adsorbent (Etim et al., 2016). Figure 2b demonstrates the influence of pH on the adsorption efficiency of the CFs aerogel. The adsorption capacity is determined in the range of 8.45-11.52 mg/g. The dye removal increases from 67.67 to 92.20 % with increasing pH from 3 to 7. Because the pH_{zpc} of the CFs aerogel equals 6.8, the aerogel's surface is positively charged in acidic solutions ($pH < pH_{zpc}$). The hydroxyl groups of the aerogel are protonated, resulting in the repulsion force between the cationic MB molecules and the CFs aerogel. In a neutral aqueous medium, the number of negatively charged surface positions on the adsorbent increases and leads to a rise in cationic dye adsorption because of a strong electrostatic force. The efficient elimination reaches a peak at pH 7 and then begins to drop slightly. In higher alkaline conditions, the CFs aerogel has competed with OH^- ions in the solution to attack the active sites of the cationic dye. Due to the high porosity and amount of negatively charged groups, the competition is overpowered by the adsorbent, thus, a decline in adsorption is a relatively slight difference. A similar tendency is obtained from cationic dye removal by Sago pith cellulose nanofibril aerogel (Jeng et al., 2020). From Figure 2b, pH 7 is selected to study the MB sorption kinetics of the CFs aerogel.

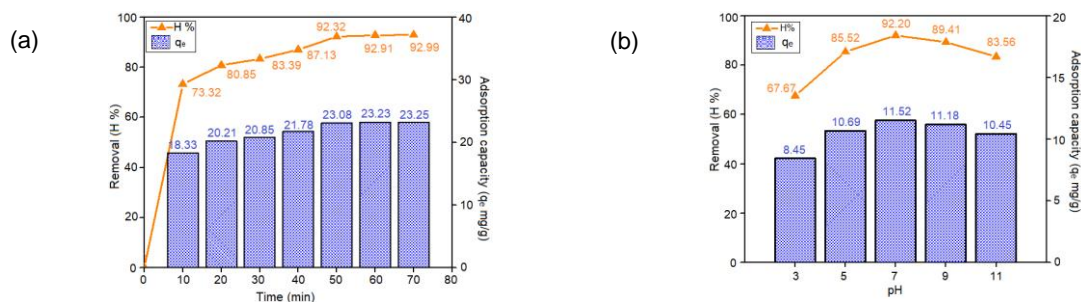


Figure 2: Effect of (a) contact time, (b) pH on adsorption capacity of the CFs aerogel

3.2.3 Initial MB concentration

Figure 3a shows an initial MB-dependent adsorption behaviour of CF aerogel. When the primary MB content increases (12.5-100 mg/L), the adsorption capacity enhances as well (5.74-43.84 mg/g). At lower MB concentrations (12.5 and 25 mg/L), the gradient concentration causes a rapid rise in the adsorption capacity, the adsorption curve has a large slope. Higher than 25 mg/L MB solution, MB elimination decreases from 95.73 to 87.68 % if the initial MB concentration continuously increases. The impact of the primary dye concentration is associated with the instant correlation of both the MB concentration and free link positions on the bio-sorbent surfaces. When initial dye concentrations increase, the removal ability of dye on aerogel decreases. This may be due to the saturation of adsorption sites on the CFs aerogel's surface (Jeng et al., 2020).

3.2.4 Adsorption kinetics

As seen from Figure 3b and Table 1, the R^2 value of the pseudo-second-order model is higher than that of the pseudo-first-order model in two experiments with different initial MB concentrations of 25 and 50 mg/L. The q_e values calculated results from the pseudo-second-order model (12.35 and 23.25 mg/g for MB concentrations of 25 and 50 mg/L) are almost as same as the experiment results (12.53 and 24.75 mg/g). The pseudo-second-order model is the best fit to describe the MB adsorption kinetics of the CFs aerogel. It also suggests that chemisorption dominates physisorption during the adsorption process (Su et al., 2020).

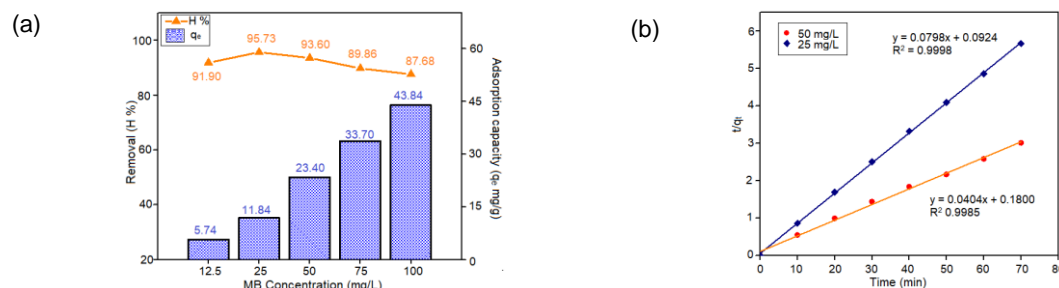


Figure 3: (a) Effect of initial MB concentration, (b) the data fitted to pseudo-second-order models

Table 1: Parameters of two kinetic models

Initial MB conc.	pseudo-first-order model			pseudo-second-order model		
	q_1	k_1	R^2	q_2	k_2	R^2
25	6.334	0.01120	0.6334	12.53	0.06890	0.9998
50	6.033	0.06780	0.5801	24.75	0.00910	0.9985

3.2.5 Adsorption isotherms

The adsorption isotherm is especially important for the representation of adsorption behaviour. It explains the essence and mechanism of the uptake are interacts between the MB molecules and the CFs aerogel. In this present paper, the investigation into the adsorption behaviour applied Langmuir and Freundlich isotherms. From Table 2 below, it can be observed Freundlich model is more relevant because of the higher R^2 value (0.9453) which almost gets 1.000. This model is applied to adsorption on heterogeneous surfaces with the interaction of adsorbed molecules (multilayer adsorption). It presumes that adsorption energy exponentially declines on the completion of the sorption centers in the adsorbent (Jeng et al., 2020).

Table 2: The Langmuir and Freundlich isotherm models

Langmuir model			Freundlich model		
k_L	q_{max}	R^2	k_F	n	R^2
0.06696	111.1	0.7462	7.760	1.342	0.9453

3.2.6 Adsorption thermodynamics

The Gibbs free energy determines the mechanism and spontaneous nature of the reaction. For MB adsorption by CFs aerogel in this study, ΔG is -2,642.61 J/mol. The negative values of ΔG predict that the physical interactions such as electrostatic forces, Vander Waal's forces, hydrogen bonding, and $\pi - \pi$ interactions may be connected with the adsorption process (Etim et al., 2016).

4. Conclusions

The bio-based aerogel from CFs for dye removal is successfully synthesized using a combination of non-toxic, biodegradable binders (PVA and XTG), and cost-effective freeze-drying. The fabricated CFs aerogel adsorbs MB with the initial concentration of 25 mg/L, effectively at pH 7, and reaches the equilibrium state after 50 min. The maximum adsorption capacity and MB removal efficiency of the aerogel are determined at 11.84 mg/g and 94.73 %. The MB adsorption of the CFs aerogel follows the pseudo-second-order and Freundlich isotherm models. The CFs aerogel has great potential in the treatment of dye-contaminated water.

Acknowledgments

This work was funded by Vingroup Joint Stock Company and supported by Vingroup Innovation Foundation (VINIF) under project code VINIF.2020.NCUD.DA112. We also acknowledge the support of time and facilities from Ho Chi Minh City University of Technology (HCMUT), VNU-HCM for this study.

References

- Ben W., Yan S., Shengnan Y., Qinghao W., Jinhua Y., 2020, Treatment of methyl blue dye wastewater solution by three dimensional electrolysis, *Chemical Engineering Transactions*, 81, 133-138.
- Etim U.J., Umoren S.A., Eduok U.M., 2016, Coconut coir dust as a low cost adsorbent for the removal of cationic dye from aqueous solution, *Journal of Saudi Chemical Society*, 20, S67-S76.
- Hiep H.D.B.T., 2018, Coconut production in the world - Prospects for Vietnam coconut industry. Retrieved from the Union of Science and Technology Associations in Ben Tre province <<http://btusta.vn/tin-tuc/1449/san-xuat-dua-tren-the-gioi-trien-vong-cho-nganh-dua-viet-nam>>, accessed 12.05.2021 (In Vietnamese).
- Jeng H.B., Teck H.L., Jin H.L., Jau C.L., 2020, Cellulose nanofibril-based aerogel derived from sago pith waste and its application on methylene blue removal, *International Journal of Biological Macromolecules*, 160, 836-845.
- Luu T.P., Do N.H.N, Le P.T.K., Duong H.M., 2020, Morphology control and advanced properties of bio-aerogels from pineapple leaf waste, *Chemical Engineering Transactions*, 78, 433-438.
- Mar'atul F., Widiyastuti, Ratna S., Heru S., 2019, Production of cellulose aerogels from coir fibers via an alkali-urea method for sorption applications, *Cellulose*, 26, 9583–9598.
- Minh D., Trong L., 2019, Vietnam coconuts are best quality in the world. Retrieved from Institute of Agricultural Science for Southern Viet Nam <<http://iasvn.org/homepage/Dua-Viet-Nam-chat-luong-nhat-the-gioi-12733.html>> accessed 12.05.2021 (In Vietnamese).
- Nga H.N.D., Viet T.T., Quang B.M.T, Kien A.L., Quoc B.T., Phuc T.T.N., Hai M.D., Phung K.L., 2021, Recycling of pineapple leaf and cotton waste fibers into heat insulating and flexible cellulose aerogel composites, *Journal of Polymers and the Environment*, 1112–1121.
- Ngoc D.Q.C., Tram T.N.N., Huong L.D.X., Nga H.N.D., Viet T.T., Son T.N., Phung K.L., 2020, Advanced fabrication and applications of cellulose acetate aerogels from cigarette butts, *Materials Transactions*, 61(8), 1550-1554.
- Quoc B.T., Son T.N., Duong K.H., Tuan D.T., Dat M.H., Nga H.N.D., Thao P.L., Phung K.L., Duyen K.L, Nhan P.T., Hai M.D., 2020, Cellulose-based aerogels from sugarcane bagasse for oil spill-cleaning and heat insulation applications, *Carbohydrate Polymers*, 228, 115365.
- Su B.K., Zhuo W., Sung W.W., 2020, Adsorption characteristics of methylene blue on PAA-PSBF adsorbent, *Chemical Engineering Transactions*, 78, 205-210.
- Zhiguo W., Shilin L., Yuji M., Shigenori K., 2012, Cellulose gel and aerogel from LiCl/DMSO solution, *Cellulose*, (19), 393–399.